Biosensors and Bioelectronics 132 (2019) 230–237

Contents lists available at ScienceDirect

Biosensors and Bioelectronics

journal homepage: www.elsevier.com/locate/bios

# Development of clay-protein based composite nanoparticles modified single-used sensor platform for electrochemical cytosensing application

Yesim Tugce Yaman[a,b,1], Oznur Akbal[a,1], Serdar Abaci[a,c,*]

[a] Advanced Technologies Application and Research Center, Hacettepe University, Ankara, Turkey
[b] Department of Chemistry, Graduate School of Science and Engineering, Hacettepe University, Ankara, Turkey
[c] Chemistry Department, Analytical Chemistry Division, Hacettepe University, 06800 Beytepe, Ankara, Turkey

ARTICLE INFO

*Keywords:*
Cancer
Composite nanoparticle
Montmorillonite
Human serum albumin
Electrochemical cytosensor

ABSTRACT

A novel sensor platform modified with clay-protein based composite nanoparticles (Mt-HSA NCs) was developed to be used in electrochemical cytosensing application for the first time. The nanocomposite synthesized with desolvation method was structurally clarified by various characterization methods. Then, the working electrode was constructed by modifying the surface of the disposable pencil graphite (PGE) with physical adsorption to perform a simple sensor system. The characterization studies proved that the Mt-HSA NCs modified surface had a biocompatible, hydrophilic and large surface area where cancer cells can easily attach to the surface. As a diagnostic method, electrochemical impedance spectroscopy (EIS), which has become very popular in recent years, was carried out. The linearity range was found as from $1.5 \times 10^2$ to $7.5 \times 10^6$ breast cancer (MCF-7) cells and the limit of detection was calculated as 148 cells $mL^{-1}$. From these results, a simple, effortless, cost effective and rapid electrochemical impedimetric sensor system for the diagnosis of breast cancer was developed by examining the interaction of Mt-HSA NCs/PGE surface with MCF-7 cells.

## 1. Introduction

Reasons for low cancer survival are the lack of biomarkers to provide early diagnosis and the development of targeted therapies. Biological markers have many possible application areas in oncology such as risk assessment, monitoring and diagnosis, differential diagnosis, prognosis determination, response of the treatment and screening progress of the illness. Circulating tumor cell (CTC), is a biomarker that can spread around cancerous tissue commonly referred to as "liquid biopsy", is known to provide real-time monitoring of tumor evolution, therapeutic activity, potential for the diagnosis and treatment of cancer (Tang et al., 2018). Kinds of strategies were developed to detect tumor cells or tissue up to now such as fluorescent imaging, molecular magnetic resonance imaging, flow cytometry, electrochemiluminescence, X-Ray radiography, immunohistochemistry, computerized tomography and so on (Hashkavayi et al., 2017; Wang et al., 2014). Nevertheless, these strategies are in general time consuming, expensive and poorly selective which suggest the development of new detection methods. Electrochemical detection strategies have attracted much attention in cancer cell research because of their outstanding advantages such as excellent portability, rapid response and sensitive recognition (Amouzadeh Tabrizi et al., 2017; Dervisevic et al., 2017; Guo et al., 2017; Hashkavayi et al., 2017). To analyze electrochemically and evaluate the cancer cells, different detection signals can be used based on current, impedance and capacitance. Among these methods, electrochemical impedance spectroscopy (EIS) provides many advantages for the detection of cancer cells such as ease of use, fast response time, high sensitivity and no need for labelling. Thus, electrochemical impedimetric cytosensors were developed using various polymer, biopolymer, nanoparticle, aptamer and peptide structures for different cancer types (An, 2016; Kavosi et al., 2015; Sun et al., 2018b; Wang et al., 2012; Yaman et al., 2018; Yazdanparast et al., 2018).

Generally, aptamer and antibody based sensors were developed for the electrochemical diagnosis of human breast adenocarcinoma cells (MCF-7) in literature (Arya et al., 2013, 2012; Hua et al., 2013; Li et al., 2011, 2010; Sheng et al., 2015; Tang et al., 2018; Yazdanparast et al., 2018; Zhu et al., 2013). However, there were also studies performed without aptamer and antibody contribution. For example, Zheng et al. developed an enzyme-free method for the diagnosis of MCF-7 cells using the enzymatic properties of nanohybrid ($Fe_3O_4$ nanocages). It was reported that the current density increased with the logarithm of the cell concentration in the range of $5.0 \times 10^1$–$1 \times 10^7$ cells $mL^{-1}$ in the

* Corresponding author at: Chemistry Department, Analytical Chemistry Division, Hacettepe University, 06800 Beytepe, Ankara, Turkey.
*E-mail address:* sabaci@hacettepe.edu.tr (S. Abaci).
[1] These authors contributed equally.

https://doi.org/10.1016/j.bios.2019.02.058
Received 1 February 2019; Received in revised form 21 February 2019; Accepted 22 February 2019
Available online 05 March 2019
0956-5663/ 

presence of 25 μM thionin (Zheng et al., 2014). Besides, a gold nanoflowers modified ionic liquid functionalized graphene based paper sensor was fabricated for the amperometric detection of MCF-7 cells by Zhang et al. (Zhang et al., 2017). A 3D microarray gold electrode modified with the polymeric structure containing benzoboric acid group instead of antibody was developed for the MCF-7 diagnosis by An et al. The LOD value was calculated as 5 cells $mL^{-1}$ by EIS method (An et al., 2018). In addition, different solid electrodes were generally used in the diagnosis of MCF-7. However, these electrodes required pretreatment such as surface polishing. Besides, the difficulty in cell diagnostics is that cells are adsorbed to the surface and the surface must be re-modified at each measurement. This situation causes the experimental process to elongate and the researcher to exert more effort. Although, most studies in the literature offered selective analysis with labelling for the diagnosis of MCF-7 cells, the development of biocompatible, unlabeled, single-used and easy prepared sensor surfaces maintain its importance. In this study, montmorillonite-human serum albumin based composite nanoparticles (Mt-HSA NCs) modified pencil graphite electrodes (PGEs) were fabricated and cytosensor application was carried out for the first time.

Kinds of materials were developed in the production of sensor platforms for high sensitivity and signal enhancement; especially clay-based nanocomposites (NCs) are only one of them. Clay-modified electrodes have gained attraction because of its high ion exchange features and unsurpassed layered design of the clay used (Fitch, 1990; Navrátilová and Kula, 2003). Montmorillonite (Mt), a smectit 2:1 phyllosilicates clay, which is hydrophilic, layered between two silica tetrahedral and one alumina octahedral sheets has high inner area, unique mucoadhesive features, with no toxicity (Mousty, 2004; Unal et al., 2017). Also, it can function as a matrix for electroactive ions as they can exhibit ion exchange properties such as polymeric ionomers (Leszczy et al., 2007). Human serum albumin (HSA) is the most ample protein in plasma, was used as an immobilization matrix for clay based NCs in this study. It is biocompatible with non-immunogenic properties and a versatile natural carrier in blood which offers potential binding sites for various materials such as metal ions, hormones, drugs and bilirubin (Heli et al., 2007). Therefore, in this study by using HSA for the construction of nanocomposites there is no need to use a label for cell detection. Mt-HSA NCs are more notable for bioanalysis due to their small size, excellent stability and biocompatibility in aqueous solution (Akbal et al., 2018).

Herein, this will be the first study of the electrochemical biosensing application of Mt-HSA NCs in which human breast adenocarcinoma cell line was used as a model cancer cell line for testing their pertinency as a cytosensor. The synthesized nanocomposite structure had high biocompatibility and high affinity to the cancer cells and thus, electrochemical detection of the cancer cells was carried out successfully. Different methods such as scanning electron microscopy (SEM), contact angle and electrochemical methods were performed for the characterization studies. The surface properties of the Mt-HSA NCs modified PGEs were revealed with these methodologies. The effect of the adsorption time of nanocomposite on the number of cells attached to the surface and immobilization time of cells were optimized. Thus, the favorable electrochemical signal was obtained in the diagnosis of MCF-7 cells. Due to the advantages mentioned above, EIS was used as a diagnostic method and a wide linear working range was obtained with low detection limit. Mt-HSA NCs based electrochemical cytosensor was developed to improve potential cancer diagnosis with low cost, biocompatible, single-used, wide detection range and good reproducibility.

## 2. Experimental

### 2.1. Reagents

For cell culture studies; disodium hydrogen phosphate, sodium chloride, Dulbecco's modified Eagle's medium (DMEM), fetal bovine serum (FBS), penicillin–streptomycin, trypsin/EDTA, 2,3-Bis-(2-Methoxy-4-Nitro-5-Sulfophenyl)-2H-Tetrazolium-5-Carboxanilide (XTT) and for nanocomposites synthesis; montmorillonite (Mt), human serum albumin (HSA) and glutaraldehyde (GA) were purchased from Sigma-Aldrich. Potassium chloride (KCl) and phosphate buffer saline were purchased from Sigma-Aldrich. MCF-7 and L929 cell lines were provided by Hacettepe University research center laboratory in Turkey. $K_4Fe(CN)_6$ and $K_3Fe(CN)_6$ were supplied from Analar Analytical Reagents and Fischer Scientific Company, respectively. All reagents were used without any modification process and were of analytical grade.

### 2.2. Instruments

All electrochemical studies were performed with *CH Instruments CHI660C* model potentiostat/galvanostat by using three-electrode configuration. Pencil graphite electrode (PGE) was used as a working electrode; a silver/silver chloride (Ag/AgCl, 3 M KCl) and a platinum (Pt) wire were used as a reference and counter electrode, respectively. The preparation of PGE was described in our previous study (Yaman and Abaci, 2016).

Mt doped HSA nanocomposites were characterized with attenuated total reflectance fourier transform infrared spectroscopy (ATR-FTIR), dynamic light scattering (DLS), contact angle, scanning electron microscopy (SEM), energy-dispersive X-ray spectroscopy (EDX) and ultraviolet–visible (UV–vis) spectroscopy. ATR-FTIR studies were performed to identify the chemical structure of HSA and Mt-HSA nanocomposites using Nicolet TM ISTM 50 spectrometer (Thermo Fisher Scientific, USA). The spectra were conducted between 4000 $cm^{-1}$ and 600 $cm^{-1}$. SEM was studied to evaluate the morphology of nanocomposites and modified electrodes, and EDX was performed to prove the internalization of Mt into nanocomposites. SEM-EDX analyses were performed by using a 10 keV electron beam, produced by a Tescan GAIA 3 FIB-SEM microscope (Czech Republic). To prepare the samples, 5 μL of nanocomposites was dropped on silicon wafers, covered with gold after drying with nitrogen gas. DLS studies of the nanocomposites were evaluated by a Zetasizer Nano ZS instrument (Malvern Instruments, UK). The records were performed in water at 25 °C and 173° backscatter angle. The contact angles which evaluate wettability of a surface were measured the liquid nanocomposite droplet profile deposited on a solid surface. A calibrated micro-syringe was used to place a drop of ultrapure water on the substrate surface which contained nanocomposites. A camera connected to an optical microscope recorded the drop-substrate interface image. UV–vis studies were performed to confirm HSA and Mt in the nanocomposite structure by UV–vis spectroscopy (Shimadzu, Japan) at room temperature between 190 and 800 nm.

### 2.3. Synthesis of Mt-HSA nanocomposite

The self-assembled Mt-HSA nanocomposites were synthesized by desolvation method described previously (Akbal et al., 2018). Briefly, nanosized Mt solution was prepared under sonic prop with 90% amplitude, 20 kHz frequency and then mixed with the HSA solution (30 mg $mL^{-1}$). To cross-link the amine ends of lysine in HSA structure and hydroxyl group of Mt glutaraldehyde was added to the Mt-HSA solution after the dropwise addition of ethanol. The solution was kept at 25 °C under stirring for overnight. In the last stage, the nanocomposite suspension was washed twice at 12000 rpm for 30 min and resuspended in 1 mL distilled water.

### 2.4. Cell culture

MCF-7 human breast adenocarcinoma cell line was cultivated under 5% $CO_2$ atmosphere at 37 °C. DMEM, 10% FBS and 1% penicillin-streptomycin were used as a cell medium. The cells were gathered after

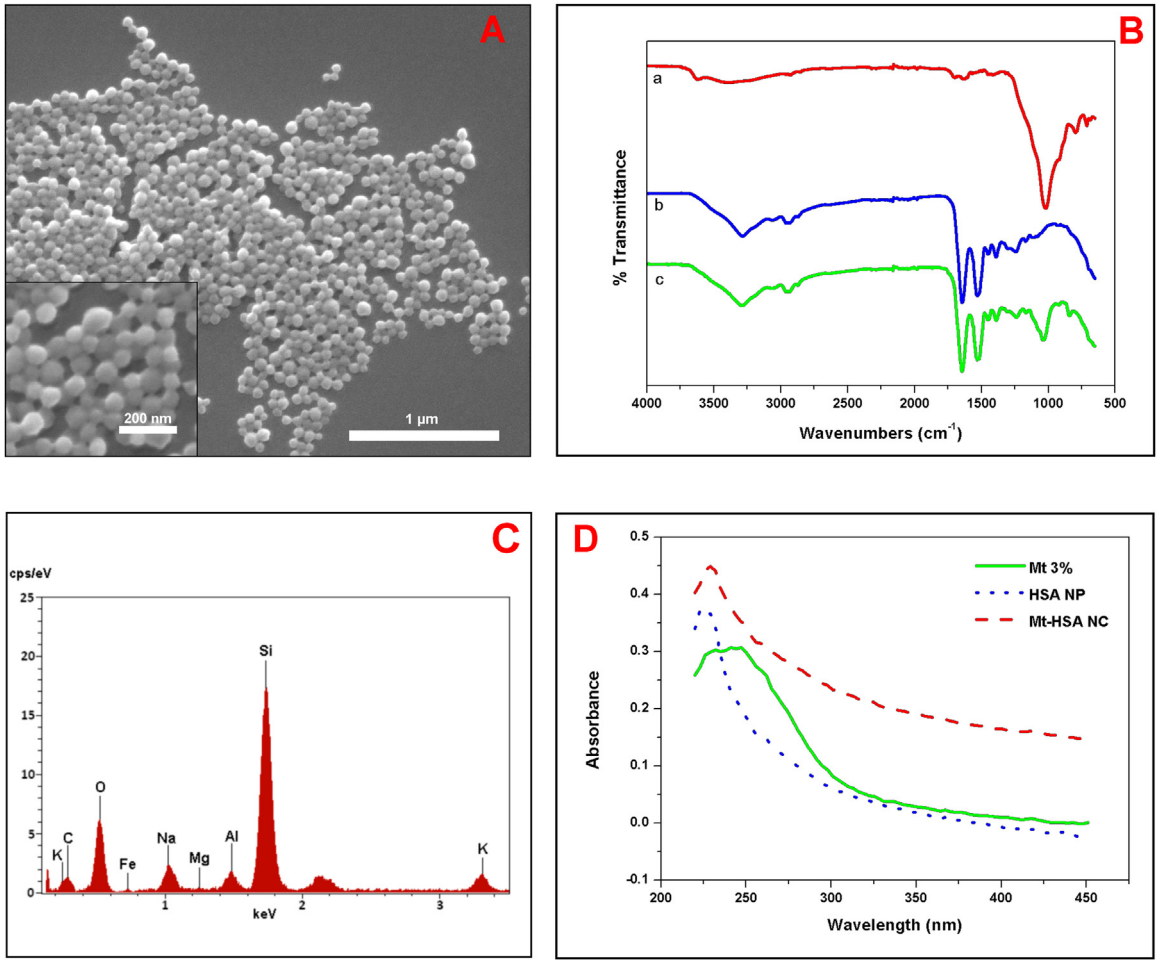


**Fig. 1.** A) SEM image of Mt-HSA NCs, scale bar: 1 µm, B) ATR-FTIR spectrum of a) Mt, b) HSA NP, c) Mt-HSA NCs, C) EDX spectrum of Mt-HSA NCs, D) UV–Vis spectrum of Mt, HSA NP and Mt-HSA NCs.

reaching 70% confluency. To prepare the cells, first all medium was removed then washing with phosphate buffer solution (PBS) and harvested with 0.25% trypsin/EDTA solution from the flask surface. Afterward, PBS was added to trypsinized cell. The cells were centrifuged at 4000 rpm for 2 min and purified twice to remove the unwanted additives. Lastly, the cell suspension was prepared with PBS (Wahab et al., 2014). All materials and equipment were purified under UV light and all experiments were performed in the biological safety cabinet to prevent contamination.

### 2.5. Modification and immobilization step

The Mt-HSA NCs modification was easily carried out with the passive adsorption on the sensor surface. Mt-HSA NCs solutions prepared in water at a concentration of 3 mg $mL^{-1}$ were taken to tubes and PGEs were kept in these solutions for 1 h (optimum adsorption time). The modified electrode was referred as Mt-HSA NCs/PGE. Then modified electrode surfaces were washed for 2 s in ultra-pure water solution and allowed to dry at room temperature. MCF-7 cells were in PBS and Mt-HSA NCs/PGEs were dipped in this solution for 120 min (optimum immobilization time). The electrode surfaces were washed for 2 s in PBS and allowed to dry in an oven at 37 °C.

### 2.6. Biocompatibility of PGE

The biocompatibility of the PGEs with and without Mt-HSA NCs were evaluated by XTT assay on MCF-7 and L929 cell lines. The assay was carried out according to manufacturer's instructions. To begin, both cell lines were incubated with DMEM and 10% FBS at 37 °C under 5% $CO_2$. The cells were collected after reaching the desired confluency. After the cells were harvested with 0.25% trypsin/EDTA solution they were centrifuged at 4000 rpm for 2 min and resuspended. The cells were sown with an amount of $5 \times 10^3$ cells/well in a 96-well culture plate and preserved for overnight. On the other hand, bare and Mt-HSA NCs/PGEs were organized and sterilized with UV light. Then, the sterilized materials were settled in DMEM without FBS and kept at 37 °C for 72 h. The sample extracts were placed on the cells and conserved for 24 h under storage conditions (Kostoryza et al., 1999). After that, XTT solution (100 µL) was added to each well which include the extract containing medium and incubated for another 4 h at 37 °C. The absorbance was recorded at 475 and 660 nm using UV–vis spectrophotometer, and the cell viability was calculated with Eq. (1) (Uzunoglu et al., 2010).

$$Specific\ Absorbance = A475\ nm\ (Assay) - A475\ nm\ (Blank) - A660\ nm\ (Assay) \quad (1)$$

### 2.7. Electrochemical Characterization and Detection

Electrochemical characterization of the bare, modified PGE surfaces are generally performed with cyclic voltammetry (CV) and electrochemical impedance spectroscopy (EIS) methods in solutions containing redox probe. CV method was used to monitor the electrochemical signal change of the modified PGEs, cyclic voltammograms

were recorded in the solution containing the 5.0 mM $Fe(CN)_6^{3-/4-}$ (0.1 M KCl) as a redox probe was scanned at 100 $mVs^{-1}$ in the range of − 0.3 to 0.8 V (vs. Ag/AgCl). Besides, in order to demonstrate the interaction of the MT-HSA NCs/PGEs with the MCF-7 cells, cyclic voltammograms were performed in the range from 0.0 V to 1.3 V (vs. Ag/AgCl) at the scanning rate of 50 $mVs^{-1}$ in 0.1 M PBS (pH 7.0). To characterize bare-modified PGE surfaces and diagnose MCF-7 cancer cells, EIS method was used in the frequency range of 0.1 kHz to 1.0 MHz with 10 mV amplitude alternating wave in the solution containing 5.0 mM $Fe(CN)_6^{3-/4-}$ (0.1 M KCl) redox probe. The calibration range was correlated using the $\Delta R_{ct}$ ($\Delta Rct = R_{ct(MCF\text{-}7\ cells\ on\ Mt\text{-}HSA\ NCs/PGE)} - R_{ct(Mt\text{-}HSA\ NCs/PGE)}$) value indicating the resistance change at the electrode/solution interface by fitting the Nyquist plots.

## 3. Results and discussion

### 3.1. Characterization of clay-protein based nanocomposite

Spherical and monodisperse Mt-HSA nanocomposites were synthesized by self-assembly process which further cross-linked with glutaraldehyde (GA). GA reacts with amine ends of the lysine amino acid in the structure of HSA at neutral pH through Schiff base (-C=N-) formation which is stable under the crosslinking conditions (Langer et al., 2008; Yan et al., 2015). Protein-clay nanocomposites can be synthesized by direct mixing of two aqueous solutions including protein and clay suspension. The obtained material is called an ex-situ nanocomposite. The majority of the protein was located outside the clay ranges (Valapa et al., 2017). Here, Mt solution was mixed with HSA and cross-linked with GA. SEM images demonstrated that the homogenous dispersed and spherical nanocomposites were synthesized (Fig. 1A) which also supported by DLS results. According to DLS, the average diameter of Mt-HSA NCs was nearly 77 ± 3 nm with a good polydispersity index and the zeta potential was recorded as − 20 mV.

Fig. 1B represented the ATR-FTIR spectra of Mt, HSA NPs and Mt-HSA NCs. For all the samples, the spectrum of Mt demonstrated a broadened Si-O-Si stretching band at 1005 $cm^{-1}$ and O–H stretching band at 3633 $cm^{-1}$. These bands can be used for the identification of Mt. The same band was also seen with a small shift in the spectrum of Mt-HSA. In addition, 870 $cm^{-1}$ assigned to Si-O-Al stretching, while 1634 $cm^{-1}$ was H-O-H bending which also presented in Mt-HSA NCs spectrum (Bagchi et al., 2014). In HSA NPs spectrum, the band at 1655 $cm^{-1}$ and 1510 $cm^{-1}$ displayed C=O stretching of amide-I and C-N stretching coupled with N-H bending of amide-II, respectively which showed secondary structure of HSA that also presented in Mt-HSA NCs (Charbonneau et al., 2009). ATR-FTIR analysis results showed that Mt-HSA NCs was successfully reconstructed and can be used in further experiments.

Mt contains oxygen (O), iron (Fe), magnesium (Mg), aluminum (Al), silicon (Si), and potassium (K) which also demonstrated in EDX analysis of Mt-HSA NCs (Fig. 1C) proved that Mt was doped successfully to nanocomposite.

The absorption spectra of Mt, HSA NP and Mt-HSA NCs were shown in Fig. 1D. HSA showed absorption peaks at around 225 and 260 nm. The strong absorption peak (225 nm) revealed the absorption of the backbone of HSA while the weak peak (260 nm) reflected from the aromatic residues of HSA NPs. Mt demonstrated an absorption band at 262 nm that can be attributed to $Fe^{3+}$ ions in octahedral construction. In Mt-HSA NCs, the shift at 262–260 nm was resulted because of $O^{2-}$ ions inside the octahedral structure of Mt. The transition at 225 nm remained at the same energy (Vijayakumar and Rao, 2012).

### 3.2. Characterization of Mt-HSA NCs/PGE

To examine the effect of the modification step on surface properties, microscopic, electrochemical and contact angle methods were performed. In Fig. 2A, SEM images were given for the bare, modified and cell immobilized PGE surfaces. It was observed that there were irregular graphite layers on the surface of the bare PGE as expected. The surface was modified by Mt-HSA NCs with physical passive adsorption method and this step retained its original spherical shape. This modified layer was observed as homogeneous (Fig. 2B). After cell immobilization step onto Mt-HSA NCs/PGE, it was observed that MCF-7 cells with a size of approximately 20 μm and irregular shape adhered to the surface successfully in Fig. 2C.

Fig. 2D demonstrated that the contact angle images of Mt, HSA NP and Mt-HSA NCs on the surface of PGE, corresponded to 35.29°, 42.22°, and 21.99°, respectively. The Mt-HSA NCs represented a notably abated contact angle (θ) due to the hydrophilic properties of the Mt-HSA NCs modified PGE surfaces. The Mt contributed to the self-assembly formation of the NCs and changed the features of the resulting Mt-HSA NCs, such as modifying the surface functional groups and performing more hydrophilicity with respect to the each single materials. The hydrophilic nanocomposites maintained a suitable micro surface for adhering cells, which is vital for the establishment of an electrochemical cytosensor (Lian et al., 2017).

Cyclic voltammetry (CV) and electrochemical impedance spectroscopy (EIS) are often utilized for the investigation of the surface properties at each modification step to construct electrochemical sensors. Therefore, cyclic voltammograms of the bare and modified electrodes were analyzed in the medium containing ferricyanide/ferrocyanide redox probe ($Fe(CN)_6^{3-/4-}$).

As can be seen in Fig. 3A, it was determined that the peak currents of the redox pair increased after the Mt-HSA NCs modification. Also, the peak voltage values approached each other which mean the reversibility was better than bare surface. Based on these results, it can be concluded that the reduction/oxidation reaction of the redox pair required less energy by the modification process. The results were given in Supplementary Table 1. The electroactive area of the electrode surfaces were determined by Randles-Sevcik equation using the peak current values obtained from the cyclic voltammograms (Bolat et al., 2018). The electroactive surface area of the bare and modified electrode was calculated as 0.184 $cm^2$ and 0.281 $cm^2$, respectively. The Mt-HSA NCs which adsorbed to the surface caused an increase in the surface area of the PGE. EIS was used as a complementary method and Rct values expressing electrode/solution interface resistance were calculated by using Randles circuit (inset of Fig. 3B). The Rct values were determined of bare and Mt-HSA NCs/PGE as 494.2 ± 83.28 and 124.9 ± 10.91, respectively. The lower Rct value indicated that the modified surface increased the electron transfer rate which was compatible with CV.

Besides, in order to show the electrochemical stability of the developed surface, cyclic voltammograms were taken for 50 cycles in the same condition of Fig. 3. As can be seen from the voltammograms, it was determined that there was a slight decrease in the peak currents of the redox probe after 50 cycles (Supplementary Figs. S1). We thought that this experiment proved the good stability of the developed surface.

### 3.3. Biocompatibility study of the cytosensor

The biocompatibility of cytosensor surface especially for the viability of cells is a critical factor for electrochemical detection of cells. Therefore the electrode component should demonstrate high biocompatibility or low toxicity for alive cells. XTT test, an assay of evaluating the cytotoxicity of materials in cell culture, was performed to assess cell viability as a function of redox potential. The control cells were assumed as 100% viability. Toxic effect of the electrode materials was evaluated according to cell viability with respect to control group. According to XTT assay results, after 24 h treatment, no cytotoxic effect was seen with both materials (bare and Mt-HSA NCs modified PGEs) (Supplementary Figs. S2).

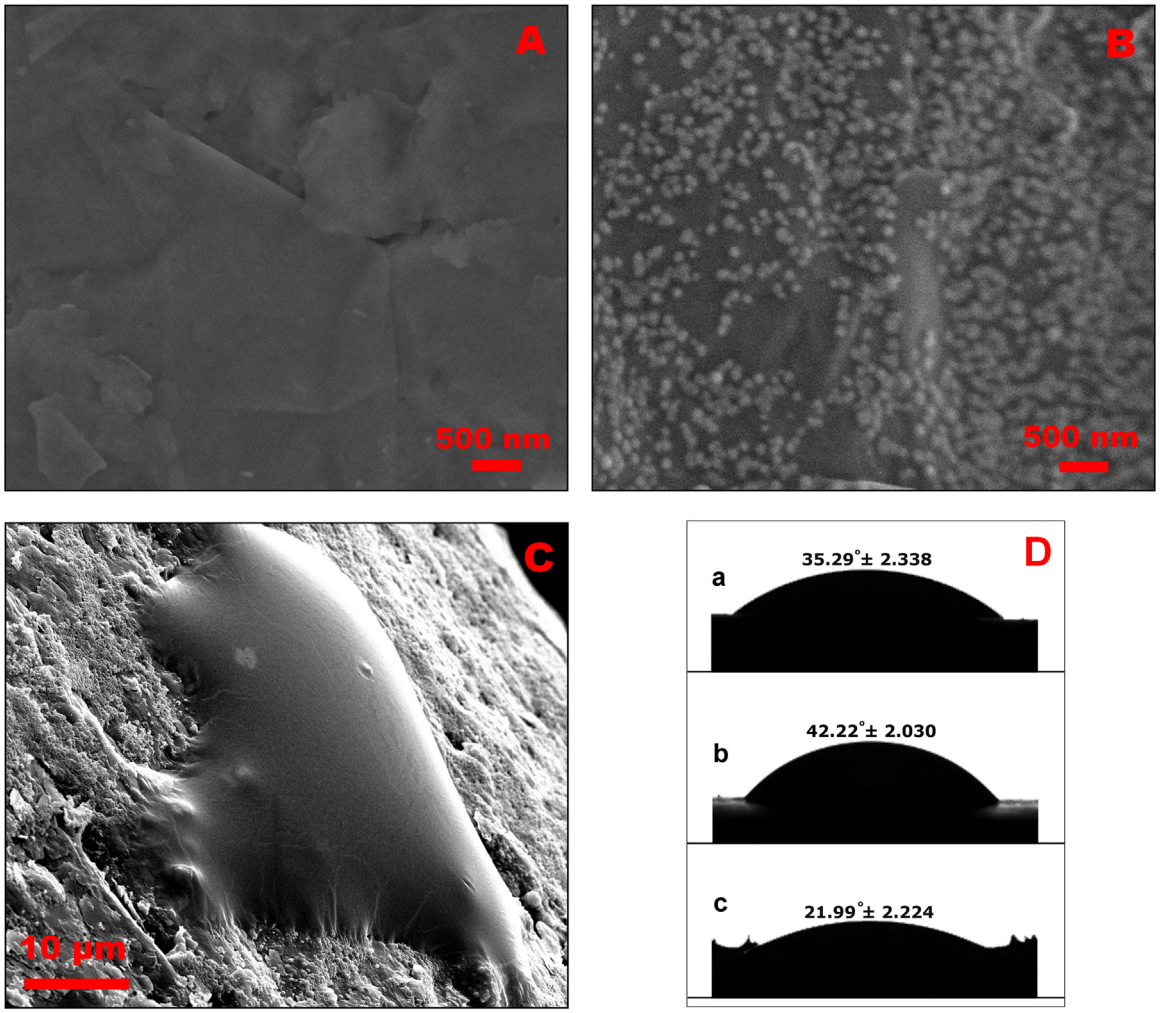


**Fig. 2.** SEM images of A) Bare PGE, B) Mt-HSA NCs modified PGE, C) MCF-7 cells immobilized onto Mt-HSA NCs modified PGE, D) Contact angle images of a) Mt, b) HSA NP, and c) Mt-HSA NCs on the surface of PGE.

### *3.4. Investigation of the interaction of MCF-7 cells with Mt-HSA NCs/PGE*

After the immobilization of MCF-7 cells onto Mt-HSA NCs/PGE surfaces, cyclic voltammograms were recorded to examine the electrochemical behavior of the MCF-7 cells (Fig. 4A). In Fig. 4 A.b, two irreversible oxidation peaks were obtained in the voltammogram of the MCF-7 immobilized Mt-HSA NCs modified PGE.

Guanine oxidation was observed at about 0.68 V (vs. Ag/AgCl) as an indicator of effective cell immobilization due to cell viability. In addition, Mt-HSA NCs supported the electron transfer between the electroactive cell center and the electrode surface and thus oxidation of adenine in the cell cytoplasm was observed at about 0.95 V (vs. Ag/

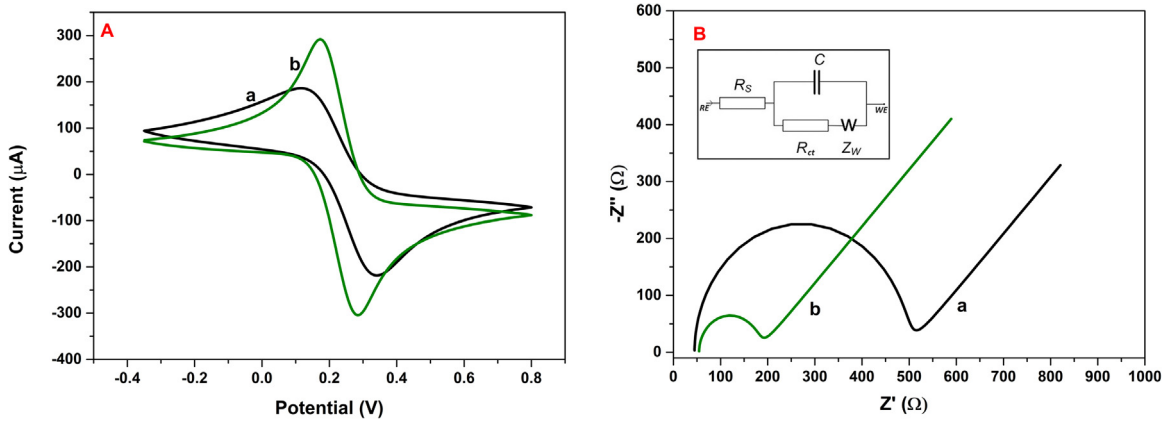


**Fig. 3.** A) Cyclic voltammograms of a) bare and b) Mt-HSA NCs modified PGE in containing 5 mM $Fe(CN_6)^{3-/4-}$ redox probe (0.1 M KCl) solution. Conditions: $E_{initial\ (i)}$: − 0.3 V $E_{final\ (f)}$: 0.8 V (vs. Ag/AgCl) scan rate (SR): 100 $mVs^{-1}$. B) Nyquist diagrams of a) bare and b) Mt-HSA NCs modified PGE. Inset demonstrates the Randles circuit elements; Rs: the electrolyte resistance, Cdl: double-layer capacitance, Rct: the electron transfer resistance, Zw: the Warburg impedance.

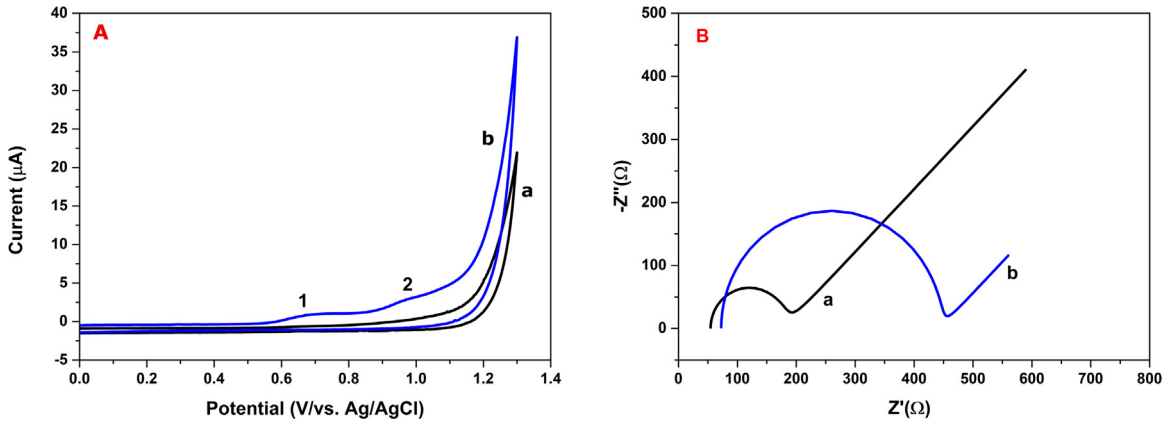


**Fig. 4.** A) Cyclic voltammograms of a) Mt-HSA NCs/PGE, b) $5.0 \times 10^3$ cells $mL^{-1}$ MCF-7 immobilized on the Mt-HSA NCs/PGE in pH 7.0 PBS. Conditions: $E_i$: 0.00 V-$E_f$: 1.30 V (vs. Ag/AgCl), SR: 50 $mVs^{-1}$. B) Nyquist diagrams of a) Mt-HSA NCs/PGE, b) $2.5 \times 10^2$ cells $mL^{-1}$ MCF-7 immobilized on the Mt-HSA NCs/PGE (with the same conditions of Fig. 3).

AgCl) (Chen et al., 2005; Yaman et al., 2018). The Mt-HSA NCs/PGE (Fig. 4A.a) was investigated under the same conditions; cyclic voltammogram was recorded without immobilization of the cells, no peaks recorded. As can be seen from the voltammograms, the surface modification of the MT-HSA NCs provided successful immobilization of MCF-7 cells onto the electrode surface.

The interaction between the MT-HSA NCs modified sensor surface and MCF-7 cells was successfully demonstrated by the CV method. However, this method does not have sufficient sensitivity to perform the diagnosis of these cells. Therefore, this interaction was also studied with the EIS method which has been successfully applied in electrochemical diagnostics studies in recent years. For this purpose, the impedimetric spectra of Mt-HSA NCs modified PGE and cell immobilized Mt-HSA NCs/PGE were compared with each other. As mentioned above, the Rct value of the MT-HSA NCs modified PGEs was 124.9 ± 10.91. After MCF-7 cells were immobilized this surface, the resistance increased dramatically at the electrode/solution interface and Rct value increased 3-folds according to Mt-HSA NCs/PGE. Here, the MCF-7 cells prohibited the electron transfer and created a higher resistance. This result proved that EIS was a suitable method for diagnosing MCF-7 cells.

### 3.5. Optimization of modification step and cell immobilization time

The response and sensitivity of the electrochemical sensors are mostly linked with the surface modification and the conditions of experimental processes. For this purpose, the effect of adsorption time of nanocomposite on the number of cells attached to the surface was investigated. As the physical adsorption time was enhanced, the resistance of the electrode/solution interface increased. In other words, as the interaction time of the composite with the surface was increased, more cells were attached to the surface. After 60 min, however, there was a slight increase in resistance, which demonstrated that the PGEs were sufficiently covered with Mt-HSA NCs. Then, the interaction time of the cells with the surface was researched. Modified electrodes were immersed to the MCF-7 cells solution at various times and the immobilization time was optimized. When immobilization time was over 120 min or more, it was determined that the change in resistance was quite low because of the surface saturation and this period was taken as the optimum immobilization period (Fig. 5).

### 3.6. Electrochemical detection of MCF-7 cells at Mt-HSA NCs/PGE

Electrochemical impedance spectroscopy (EIS) is a technique based on the measurement of resistance affected by capacitance and inductive changes when high frequencies are applied. It is often used in electrochemical based studies to obtain information about the electrode-solution interface. Although the starting point of EIS is the characterization studies in the electrochemical sensor systems, it can also be used as a diagnosis technique alternative to voltammetric and amperometric methods in recent years due to the certain advantages. Therefore, EIS was used as a detection technique in the development of a sensitive method for electrochemical diagnosis of MCF-7 cells.

Mt-HSA NCs/ PGEs were immersed in solutions containing MCF-7 cells prepared at different concentrations and immobilized at optimum conditions. Then, the working range of the developed sensor using the ΔRct values obtained against the increasing concentration of MCF-7 cells was found. As can be seen from the graph, the sensor responded to MCF-7 cells in a wide range from $1.5 \times 10^2$ to $7.5 \times 10^6$ cells $mL^{-1}$ (Fig. 6). Limit of detection (LOD) and limit of quantity (LOQ) were calculated as 148 cells $mL^{-1}$ and 488 cells $mL^{-1}$, respectively, using the linear equation slope obtained from this graph. The number of circulating tumor cells in human blood are between 1 and 3000 $mL^{-1}$ while it is $10^9$ for erythrocyte (Sun et al., 2018a). In the light of this information, the obtained values were very useful to practical application of the developed sensor.

We also studied intra-day reproducibility of the Mt-HSA NCs/PGE. Thus, three different electrodes were modified before the measurements and exposed to the same concentration of the MCF-7 cells and then electrochemical impedance measurements were recorded. The relative standard deviation (RSD) of these measurements was found as 2.5%. This result proved that the developed sensors had reproducible responses. In addition, selectivity study was performed to show the interaction of the sensor against cancer cells was different from healthy cells. Thus, L929, which is a mouse fibroblast cell, was affected for 120 min with Mt-HSA NCs/PGE and Rct values were measured. As can be seen from the graph, Mt-HSA NCs/PGE showed more interaction with cancerous cells compared to healthy L929 cells, resulting in a higher Rct value (Supplementary Figs. S3). This result showed that the fabricated sensor can distinguish cancerous and healthy cells. The presence of cancer cells was demonstrated on the surface without any labelling. The results were compared with the literature including sensor studies that previously developed for cell sensing and some other methods. The developed cytosensor showed competing performance with them (Supplementary Table 2).

## 4. Conclusion

The Mt-HSA NCs modified PGE was tested as an unlabeled single-used electrochemical impedimetric sensor for MCF-7 cells as a cancer diagnosis platform for the first time. To characterize the morphological properties and electrochemical behaviors of the surface, different

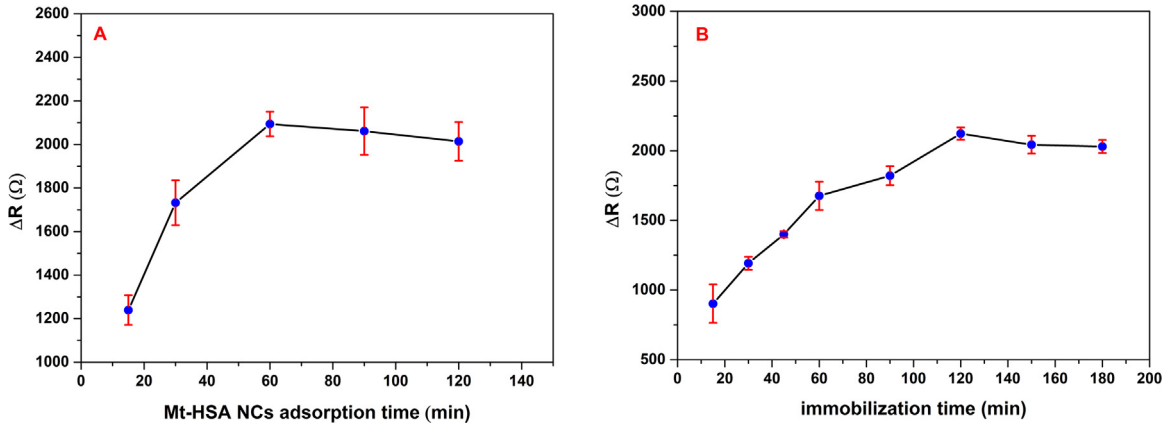


**Fig. 5.** Optimization of A) physical adsorption time of Mt-HSA NCs onto PGE surface, B) MCF-7 cells immobilization time onto Mt-HSA NCs/PGE ($3.0 \times 10^4$ cells $mL^{-1}$).

techniques were used such as SEM, ATR-FTIR, EDX, UV–Vis, contact angle and electrochemical (CV and EIS) methods. The developed cytosensor which did not need any complex amplification process or complicated operation was able to detect the cancer cells down with linear response in the range of $1.5 \times 10^2$–$7.5 \times 10^6$ cells $mL^{-1}$ and the limit of detection was determined to be 148 cells $mL^{-1}$. In addition, 50 voltammograms overlapped with the CV showed a slight decrease in the redox probe peaks and the electrochemical stability of the sensor was shown to be good. Also, RSD value was calculated as 2.5% for 3 different modified electrodes and this result showed that the developed sensors had good reproducible responses. When the obtained results were compared with current knowledge, the developed nanocomposite based sensor platform showed to be capable of competing with the literature data. The nanocomposite structure can also be used to diagnose other cancer cells by targeting with different aptamers or antibodies specific to different cancer cells. As a result, this nanocomposite stands out as a promising electrode material due to their superior properties. In future studies, it is suggested that this nanocomposite can be applied as a new sensor surface for important electrochemical applications.

## CRediT author statement

| Term | Definition |
|---|---|
| Conceptualization | Yesim Tugce Yaman, Oznur akbal, Serdar Abaci |
| Methodology | Yesim Tugce Yaman, Oznur Akbal |
| Validation | Yesim Tugce Yaman, Oznur Akbal |
| Formal Analysis | Yesim Tugce Yaman, Oznur Akbal |
| Investigation | Yesim Tugce Yaman, Oznur Akbal |
| Resources | Serdar Abaci |
| Writing – Original Draft | Yesim Tugce Yaman, Oznur Akbal |
| Writing – Review & Editing | Yesim Tugce Yaman, Oznur Akbal, Serdar Abaci |
| Supervision | Serdar Abaci |
| Project Administration | Serdar Abaci |
| Funding Acquisition | Serdar Abaci |

## CRediT authorship contribution statement

**Yesim Tugce Yaman:** Conceptualization, Methodology, Validation, Formal analysis, Investigation, Writing - original draft, Writing - review & editing. **Oznur Akbal:** Conceptualization, Methodology, Validation, Formal analysis, Investigation, Writing - original draft, Writing - review & editing. **Serdar Abaci:** Conceptualization, Resources, Writing - review & editing, Supervision, Project administration, Funding acquisition.

## Acknowledgment

The authors gratefully acknowledge the financial support of this work under ID number FDK-2018-17286 by Research Council of Hacettepe University.

## Declaration of interests

None.

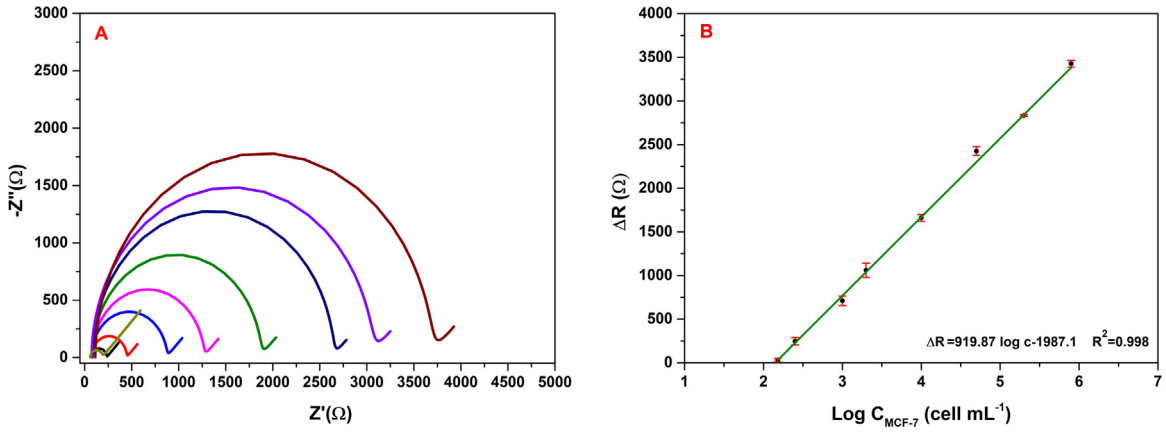


**Fig. 6.** A) Nyquist plots of developed sensor for MCF-7 cells in the concentration range from $1.5 \times 10^2$ to $7.5 \times 10^6$ cells $mL^{-1}$, B) Linear calibration graph.

## Appendix A. Supporting information

Supplementary data associated with this article can be found in the online version at https://doi.org/10.1016/j.bios.2019.02.058.

## References


Akbal, O., Vural, T., Malekghasemi, S., Bozdoğan, B., Denkbaş, E.B., 2018. Saponin loaded montmorillonite-human serum albumin nanocomposites as drug delivery system in colorectal cancer therapy. Appl. Clay Sci. 166, 214–222. https://doi.org/10.1016/j.clay.2018.09.021.

Amouzadeh Tabrizi, M., Shamsipur, M., Saber, R., Sarkar, S., Zolfaghari, N., 2017. An ultrasensitive sandwich-type electrochemical immunosensor for the determination of SKBR-3 breast cancer cell using rGO-TPA/FeHCFnanolabeled Anti-HCT as a signal tag. Sens. Actuators B Chem. 243, 823–830. https://doi.org/10.1016/j.snb.2016.12.061.

An, L., Wang, G., Han, Y., Li, T., Jin, P., Liu, S., 2018. Electrochemical biosensor for cancer cell detection based on a surface 3D micro-array. Lab Chip 18, 335–342. https://doi.org/10.1039/c7lc01117b.

An, Y., 2016. Sensitive electrochemical cytosensor based on biocompatible Au@BSA conductive architecture and lectin-modified nanoprobe. J. Electrochem. Soc. 163, B242–B247. https://doi.org/10.1149/2.1091606jes.

Arya, S.K., Lee, K.C., Dah'Alan, D. Bin, Daniel, Rahman, A.R.A.,, 2012. Breast tumor cell detection at single cell resolution using an electrochemical impedance technique. Lab Chip 12, 2362–2368. https://doi.org/10.1039/c2lc21174b.

Arya, S.K., Wang, K.Y., Wong, C.C., Rahman, A.R.A., 2013. Anti-EpCAM modified LC-SPDP monolayer on gold microelectrode based electrochemical biosensor for MCF-7 cells detection. Biosens. Bioelectron. 41, 446–451. https://doi.org/10.1016/j.bios.2012.09.006.

Bagchi, B., Thakur, P., Kool, A., Das, S., Nandy, P., 2014. In situ synthesis of environmentally benign montmorillonite supported composites of Au/Ag nanoparticles and their catalytic activity in the reduction of p-nitrophenol. RSC Adv. 4, 61114–61123. https://doi.org/10.1039/c4ra11108g.

Bolat, G., Abaci, S., Vural, T., Bozdogan, B., Denkbas, E.B., 2018. Sensitive electrochemical detection of fenitrothion pesticide based on self-assembled peptide-nanotubes modified disposable pencil graphite electrode. J. Electroanal. Chem. 809, 88–95. https://doi.org/10.1016/j.jelechem.2017.12.060.

Charbonneau, D., Beauregard, M., Tajmir-Riahi, H.A., 2009. Structural analysis of human serum albumin complexes with cationic lipids. J. Phys. Chem. B 113, 1777–1784. https://doi.org/10.1021/jp8092012.

Chen, J., Du, D., Yan, F., Ju, H.X., Lian, H.Z., 2005. Electrochemical antitumor drug sensitivity test for leukemia K562 cells at a carbon-nanotube-modified electrode. Chem. - Eur. J. 11, 1467–1472. https://doi.org/10.1002/chem.200400956.

Dervisevic, M., Senel, M., Sagir, T., Isik, S., 2017. Highly sensitive detection of cancer cells with an electrochemical cytosensor based on boronic acid functional polythiophene. Biosens. Bioelectron. 90, 6–12. https://doi.org/10.1016/j.bios.2016.10.100.

Fitch, A., 1990. Clay-modified electrodes: a review. Clay Clay Miner. 38, 391–400. https://doi.org/10.1346/CCMN.1990.0380408.

Guo, Y., Shu, Y., Li, A., Li, B., Pi, J., Cai, J., Cai, H.H., Gao, Q., 2017. Efficient electrochemical detection of cancer cells on: In situ surface-functionalized MoS2nanosheets. J. Mater. Chem. B 5, 5532–5538. https://doi.org/10.1039/c7tb01024a.

Hashkavayi, A.B., Raoof, J.B., Ojani, R., Kavoosian, S., 2017. Ultrasensitive electrochemical aptasensor based on sandwich architecture for selective label-free detection of colorectal cancer (CT26) cells. Biosens. Bioelectron. 92, 630–637. https://doi.org/10.1016/j.bios.2016.10.042.

Heli, H., Sattarahmady, N., Jabbari, A., Moosavi-Movahedi, A.A., Hakimelahi, G.H., Tsai, F.Y., 2007. Adsorption of human serum albumin onto glassy carbon surface - Applied to albumin-modified electrode: mode of protein-ligand interactions. J. Electroanal. Chem. 610, 67–74. https://doi.org/10.1016/j.jelechem.2007.07.005.

Hua, X., Zhou, Z., Yuan, L., Liu, S., 2013. Selective collection and detection of MCF-7 breast cancer cells using aptamer-functionalized magnetic beads and quantum dots based nano-bio-probes. Anal. Chim. Acta 788, 135–140. https://doi.org/10.1016/j.aca.2013.06.001.

Kavosi, B., Salimi, A., Hallaj, R., Moradi, F., 2015. Ultrasensitive electrochemical immunosensor for PSA biomarker detection in prostate cancer cells using gold nanoparticles/PAMAM dendrimer loaded with enzyme linked aptamer as integrated triple signal amplification strategy. Biosens. Bioelectron. 74, 915–923. https://doi.org/10.1016/j.bios.2015.07.064.

Kostoryza, E.L., Tonga, P.Y., Chappelowb, C.C., Eicka, J.D., Glarosa, A.G., Yourteea, D.M., 1999. In vitro cytotoxicity of solid epoxy-based dental resins and their components. Dent. Mater. 15, 363–373. https://doi.org/10.1016/S0109-5641(99)00058-5.

Langer, K., Anhorn, M.G., Steinhauser, I., Dreis, S., Celebi, D., Schrickel, N., Faust, S., Vogel, V., 2008. Human serum albumin (HSA) nanoparticles: reproducibility of preparation process and kinetics of enzymatic degradation. Int. J. Pharm. 347, 109–117. https://doi.org/10.1016/j.ijpharm.2007.06.028.

Leszczy, A., Njuguna, J., Pielichowski, K., Banerjee, J.R., 2007. Polymer / montmorillonite nanocomposites with improved thermal properties Part I. Factors influencing thermal stability and mechanisms of thermal stability improvement 453, 75–96. ⟨https://doi.org/10.1016/j.tca.2006.11.002⟩.

Li, J., Xu, M., Huang, H., Zhou, J., Abdel-Halimb, E.S., Zhang, J.R., Zhu, J.J., 2011. Aptamer-quantum dots conjugates-based ultrasensitive competitive electrochemical cytosensor for the detection of tumor cell. Talanta 85, 2113–2120. https://doi.org/10.1016/j.talanta.2011.07.055.

Li, T., Fan, Q., Liu, T., Zhu, X., Zhao, J., Li, G., 2010. Detection of breast cancer cells specially and accurately by an electrochemical method. Biosens. Bioelectron. 25, 2686–2689. https://doi.org/10.1016/j.bios.2010.05.004.

Lian, M., Chen, X., Liu, X., Yi, Z., Yang, W., 2017. A self-assembled peptide nanotube–chitosan composite as a novel platform for electrochemical cytosensing. Sens. Actuators B Chem. 251, 86–92. https://doi.org/10.1016/j.snb.2017.04.102.

Mousty, C., 2004. Sensors and biosensors based on clay-modified electrodes - New trends. Appl. Clay Sci. 27, 159–177. https://doi.org/10.1016/j.clay.2004.06.005.

Navrátilová, Z., Kula, P., 2003. Clay modified electrodes: present applications and prospects. Electroanalysis 15, 837–846. https://doi.org/10.1002/elan.200390103.

Sheng, Q., Cheng, N., Bai, W., Zheng, J., 2015. Ultrasensitive electrochemical detection of breast cancer cells based on DNA-rolling-circle-amplification-directed enzyme-catalyzed polymerization. Chem. Commun. 51, 2114–2117. https://doi.org/10.1039/c4cc08954e.

Sun, D., Lu, J., Chen, D., Jiang, Y., Wang, Z., Qin, W., Yu, Y., Chen, Z., Zhang, Y., 2018a. Label-free electrochemical detection of HepG2 tumor cells with a self-assembled DNA nanostructure-based aptasensor. Sens. Actuators B Chem. 268, 359–367. https://doi.org/10.1016/j.snb.2018.04.142.

Sun, D., Lu, J., Luo, Z., Zhang, L., Liu, P., Chen, Z., 2018b. Competitive electrochemical platform for ultrasensitive cytosensing of liver cancer cells by using nanotetrahedra structure with rolling circle amplification. Biosens. Bioelectron. 120, 8–14. https://doi.org/10.1016/j.bios.2018.08.002.

Tang, S., Shen, H., Hao, Y., Huang, Z., Tao, Y., Peng, Y., Guo, Y., Xie, G., Feng, W., 2018. A novel cytosensor based on Pt@Ag nanoflowers and AuNPs/Acetylene black for ultrasensitive and highly specific detection of Circulating Tumor Cells. Biosens. Bioelectron. 104, 72–78. https://doi.org/10.1016/j.bios.2018.01.001.

Unal, B., Yalcinkaya, E.E., Gumustas, S., Sonmez, B., Ozkan, M., Balcan, M., Demirkol, D.O., Timur, S., 2017. Polyglycolide-montmorillonite as a novel nanocomposite platform for biosensing applications. New J. Chem. 41, 9371–9379. https://doi.org/10.1039/c7nj01751k.

Uzunoglu, S., Karaca, B., Atmaca, H., Kisim, A., Sezgin, C., Karabulut, B., Uslu, R., 2010. Comparison of XTT and Alamar blue assays in the assessment of the viability of various human cancer cell lines by AT-101 (−/− gossypol). Toxicol. Mech. Method. 20, 482–486. https://doi.org/10.3109/15376516.2010.508080.

Valapa, R.B., Loganathan, S., Pugazhenthi, G., Thomas, S., Varghese, T.O., 2017. An Overview of Polymer–Clay Nanocomposites. In: Jlassi, K., Chehimi, M.M., Thomas, S. (Eds.), Clay-Polymer Nanocomposites. Elsevier, New York, pp. 29–81. https://doi.org/10.1016/B978-0-323-46153-5.00002-1.

Vijayakumar, B., Rao, G.R., 2012. PWA/montmorillonite K10 catalyst for synthesis of coumarins under solvent-free conditions. J. Porous Mater. 19, 233–242. https://doi.org/10.1007/s10934-011-9465-x.

Wahab, R., Siddiqui, M.A., Saquib, Q., Dwivedi, S., Ahmad, J., Musarrat, J., Al-Khedhairy, A.A., Shik Shin, H., 2014. ZnO nanoparticles induced oxidative stress and apoptosis in HepG2and MCF-7 cancer cells and their antibacterial activity. Colloids Surf. B 117, 267–276. https://doi.org/10.1016/j.colsurfb.2014.02.038.

Wang, R., Di, J., Ma, J., Ma, Z., 2012. Highly sensitive detection of cancer cells by electrochemical impedance spectroscopy. Electrochim. Acta 61, 179–184. https://doi.org/10.1016/j.electacta.2011.11.112.

Wang, X., Ju, J., Li, J., Li, J., Qian, Q., Mao, C., Shen, J., 2014. Preparation of electrochemical cytosensor for sensitive detection of hela cells based on self-assembled monolayer. Electrochim. Acta 123, 511–517. https://doi.org/10.1016/j.electacta.2014.01.027.

Yaman, Y.T., Abaci, S., 2016. Sensitive adsorptive voltammetric method for determination of Bisphenol A by gold nanoparticle/polyvinylpyrrolidone-modified pencil graphite electrode. Sensors 16, 756–768. https://doi.org/10.3390/s16060756.

Yaman, Y.T., Akbal, Ö., Bolat, G., Bozdogan, B., Denkbas, E.B., Abaci, S., 2018. Peptide nanoparticles (PNPs) modified disposable platform for sensitive electrochemical cytosensing of DLD-1 cancer cells. Biosens. Bioelectron. 104, 50–57. https://doi.org/10.1016/j.bios.2017.12.039.

Yan, E.-K., Cao, H.-L., Zhang, C.-Y., Lu, Q.-Q., Ye, Y.-J., He, J., Huang, L.-J., Yin, D.-C., 2015. Cross-linked protein crystals by glutaraldehyde and their applications. RSC Adv. 5, 26163–26174. https://doi.org/10.1039/C5RA01722J.

Yazdanparast, S., Benvidi, A., Banaei, M., Nikukar, H., Tezerjani, M.D., Azimzadeh, M., 2018. Dual-aptamer based electrochemical sandwich biosensor for MCF-7 human breast cancer cells using silver nanoparticle labels and a poly(glutamic acid)/MWNT nanocomposite. Microchim. Acta 185, 1–10. https://doi.org/10.1007/s00604-018-2918-z.

Zhang, Y., Xiao, J., Lv, Q., Wang, L., Dong, X., Asif, M., Ren, J., He, W., Sun, Y., Xiao, F., Wang, S., 2017. In situ electrochemical sensing and real-time monitoring live cells based on freestanding nanohybrid paper electrode assembled from 3D functionalized graphene framework. ACS Appl. Mater. Interfaces 9, 38201–38210. https://doi.org/10.1021/acsami.7b08781.

Zheng, T., Zhang, Q., Feng, S., Zhu, J.J., Wang, Q., Wang, H., 2014. Robust nonenzymatic hybrid nanoelectrocatalysts for signal amplification toward ultrasensitive electrochemical cytosensing. J. Am. Chem. Soc. 136, 2288–2291. https://doi.org/10.1021/ja500169y.

Zhu, X., Yang, J., Liu, M., Wu, Y., Shen, Z., Li, G., 2013. Sensitive detection of human breast cancer cells based on aptamer-cell-aptamer sandwich architecture. Anal. Chim. Acta 764, 59–63. https://doi.org/10.1016/j.aca.2012.12.024.